ISSN (Print) 1226-1750
ISSN (Online) 2233-6656
Journal of Magnetics 27(2), 179-185 (2022) https://doi.org/10.4283/JMAG.2022.27.2.179

Study of Change in Stainless Steel Plate Thickness using S-Domain Parameters Derived from Transient Eddy Current Oscillations Method

Yesudasu Bammidi[1], Chandra S Angani[1]*, K Sambasiva Rao[3], M. B. Kishore[4], G. Krishna Podagatlapalli[1], and S. Sreedhar[2]

[1]Department of Physics, GIS, GITAM Deemed to be University, Visakhapatnam, India
[2]Department of Mathematics, GIS, GITAM Deemed to be University, Visakhapatnam, India
[3]Department of ECE, Hindustan Institute of Science and Technology, Chennai, India
[4]Department of Mechanical Engineering, Sungkyunkwan University, Suwon, Republic of Korea

(Received 30 November 2021, Received in final form 3 April 2022, Accepted 5 April 2022)

Failures in the industrial components are unavoidable due to material degradation from various sources, thus continuous monitoring and timely inspection is mandatory for structural safety. In the present study, the recently developed Transient Eddy Current Oscillations (TECO) method is used to detect wall-thinning in a stainless-steel plate. Unlike the conventional Eddy Current Testing impedance plane data a new interpretation method has been implemented to identify a thickness variation using the S-domain parameters. Furthermore, time and frequency spectral features are analysed to get more insight into the results. The decay time and the resonant frequency are the basis for the discussion to assess the wall thickness.

Keywords : TECO system, S-domain, Decay of oscillations, Frequency, hall- sensor and stainless steel

1. Introduction

Stainless steel structures are commonly encountered element in many industries especially in the form of large pipes [1]. Steel is the constituent material for safe storage and transportation of highly corrosive substances like fluid media or gases with high pressure and temperature due to its high mechanical and chemical properties. Long-time usage of metal structures operated in harsh and ageing environment tends to degrade their properties likewise their efficiency. Local wall thinning due flow accelerated corrosion is one of the reasons that eventually results in uninvited leakages or pipeline failures [2, 3]. Therefore, to avoid sudden damage or abrupt outages in plants, a regular inspection is an essential practice to detect faults for lifetime assessment in industrial structures to attain economic benefits. This can be achieved by non-destructive testing (NDT) whose prime motive is to detect defects and asymmetries in the materials prevailing their integrity unchanged [4]. There are several basic NDT methods in use for the health monitoring of structural materials, such as Radiographic Technique (RT), Ultrasound Technique (UT), Magnetic Flux Leakage Technique (MFL) and Eddy current Testing (ECT) [5-8]. These methods are serving as the prime NDT methods for few decades. However, there are several disadvantages in these methods, for example background radiation problem in RT, coupling agent requirement in UT, the MFL is applicable only to magnetic materials and a limited depth of penetration in ECT.

Generally, the ECT can be used in many applications like material characterization, defect detection and certain metal thickness measurements, also widespread use in identifying corrosion under aircraft skin, measurement of conductivity and monitor the effects of heat treatment on materials, measurement of nonconductive coating thickness over a conductive substrate etc., [9, 10]. In view of bringing more advancement in ECT, several techniques were developed with different kinds of coil excitation methods. For example swept frequency ECT [11], pulsed ECT [12], multi-frequency ECT [13], wireless power transfer based ECT [14]. In ECT, the primary excitation coil is driven by a sinusoidal current which produces an alternating magnetic field called primary magnetic field (Φ_1). This field induces eddy currents in the test specimen underneath the coil. These induced eddy currents produce

*Corresponding author: Tel: +91-9573958184
e-mail: cangani@gitam.edu

a counter magnetic field called secondary field (Φ_2) that opposes the primary coil field Φ_1 [15]. It is well known that the induced currents are effected by several electromagnetic and mechanical factors such as, conductivity, permeability and thickness of the test material. So, one can predict the physical condition and characteristics of the test material by carefully examining the resultant magnetic field from the induced currents. Numerous sophisticated magnetic field sensors are in use to detect the resultant magnetic field, this magnetic field is nothing but the eddy current response from the test specimen. Detection coils are the commonly used sensing elements, on the other hand semiconductor magnetic field sensors such as Hall sensors and giant magnetoresistance (GMR) sensors have gained more attention and became a common choice in the contemporary research due to their compact size, high sensitivity and wide range of detection from DC to high frequencies [16-18]. In the current study, a hall sensor has been employed as a magnetic field detector, due to its linear response to an external magnetic field, easiness in handling and design of electronic circuitry.

The objective of this research is to detect a change in the thickness of a stainless steel material using a method called Transient Eddy Current Oscillations (TECO) [19]. The fundamental principle is same as the conventional ECT. However, in contrast to ECT the TECO uses a decay of oscillations instead of a continuous sinusoidal waveform to induce the eddy currents into the test object. The design of TECO probe is one of the most significant part in the system. The probe consists of a capacitor and an induction coil (excitation coil) in the driving circuitry along with a hall sensor placed at inner centre at the bottom side of the cylindrical excitation coil. There is an arrangement made in the electrical circuit that makes the capacitor to charge and discharge thorough the induction coil (excitation coil) which can generate a decay of oscillations due to exchange of energy between the two reactive elements. These under damped oscillations are introduced onto the test specimen which is underneath the probe to launch the eddy currents. The resultant response is captured by the hall sensor element and analysed in the time domain and frequency domain to extract the meaningful features.

Extracting unique features from detected response signal plays a crucial role for the understanding the obtained results for the better QNDE and which is the critical procedure in the detection of defects. There are several feature extraction and analysis methods have been proposed by the research fraternity for the assessment of structural integrity. To identify the inhomogeneity in a test material, different key features can be obtained from the data by representing either in time domain or frequency domain. For instance while applying the conventional ECT, Zeng Zhiwei *et al*., used a coil induced voltage for the representation of metallic plate thickness change [20], and Kim *et al.*, used RMS value of the sinusoidal signal to detect the far-side corrosion around a rivet in jet-engine intake [21]. Liyuan Yin *et al*., used different geometric features like width, angle and amplitude obtained from Lissajous curve (LC) for the defect detection [22]. Similarly, while applying the Pulsed ECT Angani *et al.* used the peak amplitude for the detection of local wall thickness of a stainless steel [23], G.Y Tian *et al*., used the rising point feature [24]. Yunze He *et al*., used a zero crossing point for the corrosion detection [25], Chen *et al*., proposed a descending point in the PECT response [26]. Haowen *et al*., used a feature called dynamic apparent time constant for the material thickness quantification [27]. Song *et al.*, proposed time to the last peak point feature for the detection of metal thickness [28]. In addition to time domain features, frequency domain representation of data gave more understanding on the results and analysis. For an instance, Udpa *et al.*, used the frequency domain representation [29], Qui Zhang *et al.*, used the combined representation of time and frequency features [30]. L Dura *et al*., have used the frequency domain representation and principal component analysis (PCA) for the feature extraction in wireless power transfer-based ECT [14]. Yunze He *et al*., used the frequency spectrum analysis for the detection of hidden defects [31]. Furthermore, L. Lopez *et al*., used the time-frequency analysis techniques like wavelet transform for removing ECT probe wobble noise [32] and S. Hosseini *et al*., used the time-frequency approach for the detection of hidden corrosion [33].

The previous studies on TECO method used the features like zero crossing time and the frequency shift for the detection of thickness change in the test specimen [19]. However, in the present study, the experimental data has been presented in both time and frequency domains combined in S-domain. The decay coefficient of the TECO is obtained from the envelope and the frequency of the oscillations were obtained by the FFT. The time domain feature like decay time coeffient has been used as a potential feature to interpret the specimen thickness. In addition to the frequency shift in central resonance frequency another feature which is full width half maximum (FWHM) also obtained in the present study. To get more insight on the experimental results the data has been represented in both time and frequency domain. For this purpose, the peak frequency and decay time parameters were plotted together in S-domain.

2. Experimental Setup and Working

Figure 1(a) represents the schematic diagram of the TECO system. It consists of two basic parts, first one is primary circuitry (excitation) and the other one is secondary circuit (sensing). The primary circuit consists of a voltage-source (Agilent E3632A), a relay switch, a signal generator (Agilent 3320A). The secondary circuit consists of a hall Sensor (SS49E), a differential Amplifier AD620 and a Digital Storage Oscilloscope (Key sight DSOX2014A). The TECO probe consists of a capacitor C (0.780uF) and an excitation coil L of an inductance 1.20 mH. The inductance of excitation coil was measured using a LCR meter (Scientific SM 6024). The probe is connected to a DC power supply through a relay switch. The duty of the relay switch is controlled through a function generator. Probe is one of the major components in the circuit which is used to detect the resultant magnetic field from the test specimen. For this purpose, a hall sensor kept inside the excitation coil at the bottom side of the cylindrical centre, by placing the hall sensor in such a way it faces the surface of the test specimen.

A differential amplifier circuit was designed with a gain factor of ~50 (given by the equation Gain = (49.4 kΩ/ R_G)+1) to measure the sensing voltage from the hall sensor, where the voltage measured is proportional to the sum of the primary and secondary magnetic fields which are perpendicular to the sensing area of the hall sensor. Initially, the capacitor in the probe charged by switching ON the relay using the function generator which generates a 6 V pulses of 50 % duty cycle with the repetition rate of 1 s. When the relay is ON then the DC power supply connected to the capacitor C. Similarly when the relay is OFF then the capacitor discharges through inductor which creates a decay of oscillations.

2.1. Basic principle and data acquiring

As seen in the circuit diagram in Figure 1(a), during the positive half cycle of the signal from function generator (6 V), the relay switch turned to ON state enables a path for charging the capacitor. The DC voltage source supplies the energy to the capacitor to fully charge it. After a while (0.5 s), the pulse voltage from function generator becomes 0 V, the relay goes to OFF, now the capacitor discharge

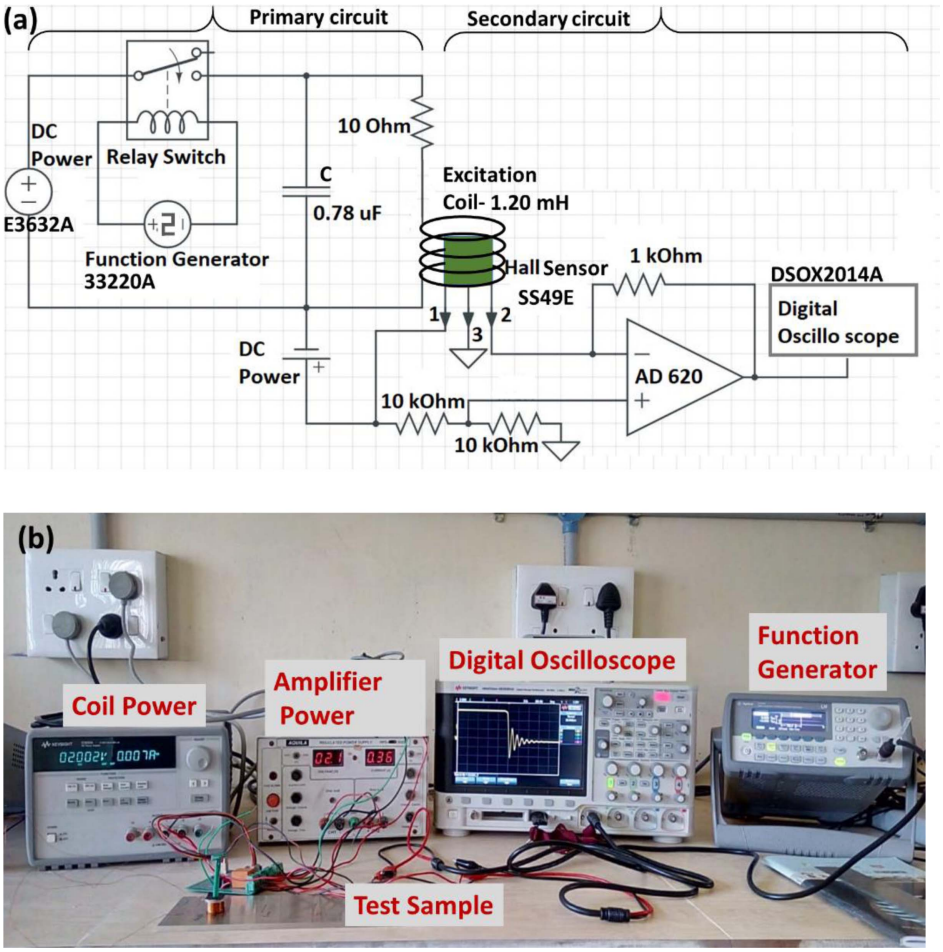

Fig. 1. (Color online) (a) Schematic diagram of TECO system, (b) Photograph of laboratory TECO system.

the voltage through the inductor coil which is connected in parallel to the capacitor. This discharging of capacitor create a free running damped oscillations at resonance frequency given by $1/2\pi\sqrt{LC}$, where L and C are the inductance and capacitance of the probe, respectively. These decay of oscillations create a time varying current in inductor which produces time varying magnetic field. By placing the probe on the conductive specimen, the magnetic field induces the eddy currents in the specimen. To detect the decay of oscillations a hall sensor is placed in the excitation coil.

From the above discussion it is clear that the oscillations are created when the relay is OFF, hence the data was obtained during the negative edge of the function generator pulse signal i.e. immediately after switching OFF the relay. To simulate the thickness change in steel material a homogeneous test specimen of stainless steel (SS304) was prepared with different thicknesses of 1, 2, 3, 4 and 5 mm. The test specimen has the total length of 250 mm and the width of 50 mm. The experimental data is obtained from the probe by placing it on each thickness of the test specimen.

3. Results and Discussions

3.1. Work flowchart

The flow chart in the Fig. 2 is the process of steps involved for analysing the TECO signal. After reading the data from the probe by placing it on the different thicknesses of the test specimen, the data must be pre-processed using signal smoothening technique for removing the noise in the signal. After pre-processing, the envelopes of the decay of oscillations for each thickness are determined, and their decay coefficients (σ) have determined by using exponential curve fitting. On the other hand, Fast Fourier Transformation (FFT) has been calculated to observe the pattern of the frequency shift in the signal with a change in the test specimen thickness. Finally, the results are plotted by taking the decay coefficient σ on X-axis and the angular frequency ω on Y-axis.

3.2. Decay of oscillations

The probe is nothing but a tank circuit with an excitation coil L and C. The parallel combination of the capacitance and the inductance can be represented by a second order differential equation [34]. The solution for an instantaneous current of the decay of oscillations can be represented by an equation given below.

$$i(t) = I_o e^{-\sigma t}\cos(\omega t) \quad (1)$$

Where $i(t)$ is the instantaneous amplitude of current, I_o is the current at time $t = 0$, σ is the damping coefficient and ω is the angular frequency of free running oscillations.

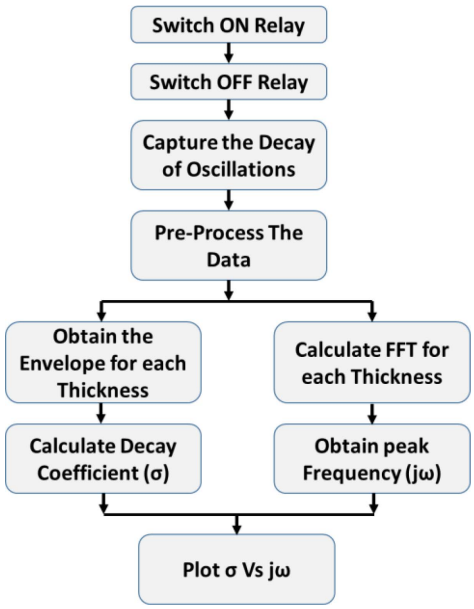

Fig. 2. Flowchart of the data analysis from the TECO system.

Figure 3(a) shows the experimental results obtained from the probe on different thicknesses of the test specimen. Different features are extracted after analysing the decay of oscillations. Firstly, the envelope of the measured signal shown in Fig. 3(b), the second one is the Full Width Half Maximum (FWHM) as shown in Fig. 3(d) obtained from normalized FFT of the response signals from various thicknesses of the test specimen.

It is well known that a change in the properties of conductive metal causes a change in secondary magnetic field that originated from the induced eddy currents, it leads to a change in impedance of the probe [35]. Impedance is the function of resistive (R) and reactive (X_L) components of a coil, thus a change in coil impedance may be the result of any of these two parameters. For instance, the inductance of the coil decreases, and its resistance increases by placing it on non-ferromagnetic electrically conductive material [35, 36]. The change in inductance causes a significant shift in the resonance frequency according to the relation $1/2\pi\sqrt{LC}$, as shown in Fig. 3(c). There is only a certain amount of eddy currents induced in a given volume of material [36] within the range of a standard depth, it means, a thicker material supports more induced currents than thinner material. Thus, the thicker part of the sample can accommodate more eddy currents which causes more secondary magnetic field, which results in the decrease in the resultant field detected by the sensor. Hence the amplitude and the decay time of oscillations

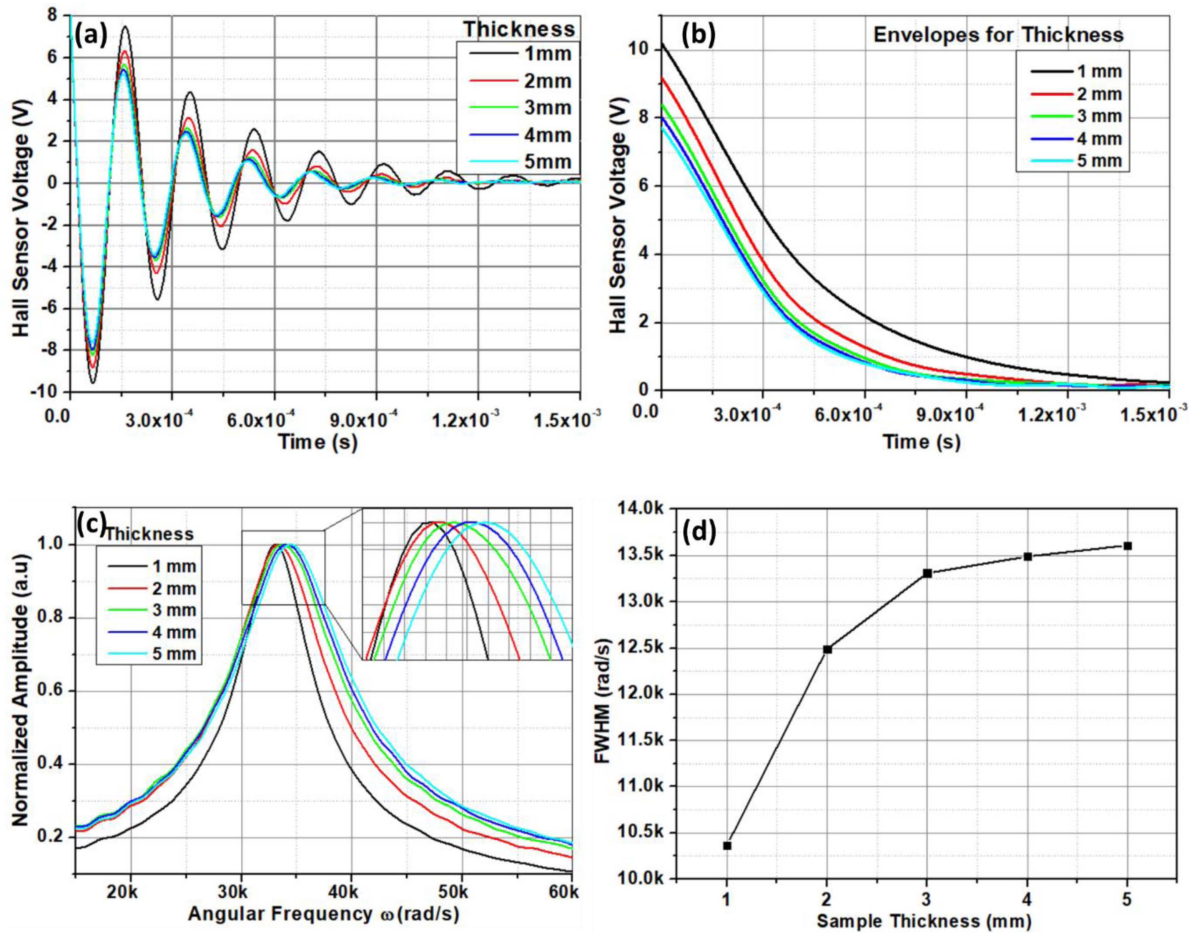

Fig. 3. (Color online) (a) TECO response with increasing thickness (b) envelopes of the TECO response at different thicknesses of test specimen (c) Normalized FFT for TECO signal (d) Full Width Half Maximum (FWHM) for normalized FFT on each thickness of test specimen.

reduced as shown in Fig. 3(b). This quick decay of oscillation caused the broadening of FFT response, it caused the increase of FWHM as shown in Fig. 3(d).

3.3. S-Domain representation

Keeping simple data representation methods in mind, just like impedance plane representation of conventional ECT in all the commercial equipment, we propose the S-domain representation of TECO data. The S-domain or S-plane is a complex plane on which Laplace transforms are graphed. The Laplace transform is used to transform a function from the time-domain into the S-domain [37]. A real function $f(t)$ is translated into the S-plane by taking the integral of the function multiplied by e^{-St} from 0 to ∞ where S (S = σ + $J\omega$) is a complex quantity.

$$F(s) = \int_0^{\infty} f(t)e^{-St}dt \tag{2}$$

Where $F(s)$ is the Laplace transform of the function $f(t)$. The Laplace transform of the decay of oscillations is represented by equation (2) considering I_o = 1.

$$F[e^{-\sigma t}\cos\omega t] = \frac{s+\sigma}{(s+\sigma)^2+\omega^2}$$

The poles of the above system of equation can be obtained by the roots of the denominator.

$$(s+\sigma)^2 + \omega^2 = 0$$

$$(s+\sigma) = \pm j\omega$$

$$s = -\sigma \pm j\omega \tag{3}$$

The S-domain plot has been shown second quadrant on the positive side of the imaginary axis (though there is $\pm j\omega$), for each thickness of the test specimen, the values of σ and $j\omega$ are plotted in complex plane. The decay coefficient σ is obtained from the decay envelope curve as shown in Fig. 4(a). As sown in the above Fig. 4(b) the data is clearly shows the significant change in real and

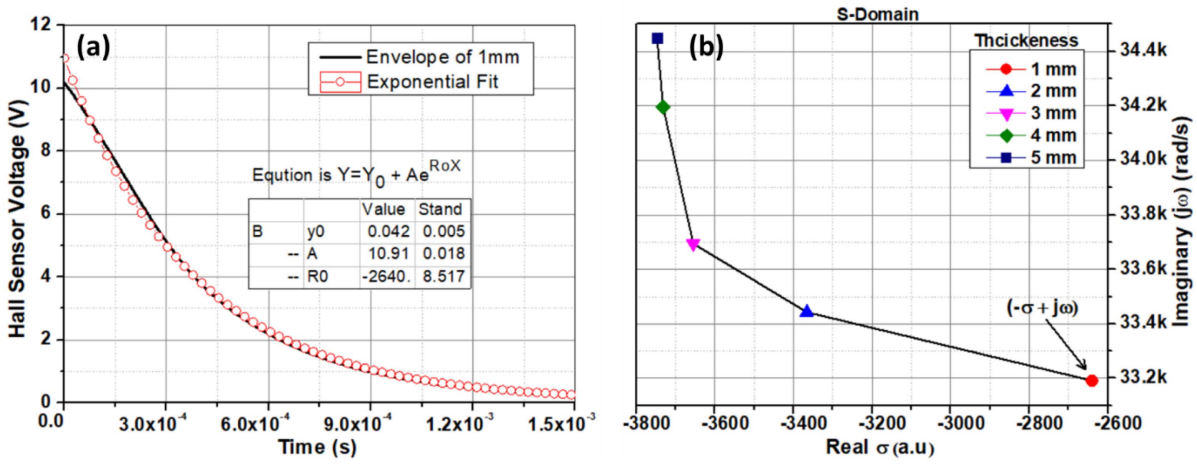

Fig. 4. (a) Exponential fitting of envelope to obtain the decay coefficient (b) S-domain Representation of the Poles of the Laplace solution of exponential decay.

imaginary components for each thickness of the specimen. The change in σ is caused by the quick decay of the oscillations and the change in $j\omega$ is caused by the shift in the resonant frequency due to change in thickness of the test specimen.

4. Conclusions

In the present study, a new Non-Destructive Testing (NDT) method, called Transient Eddy Current Oscillations (TECO) method is used to address a local wall-thinning in a stainless steel plate. Experiments were conducted on a thick specimen with changing thickness from 1 mm to 5 mm with 1 mm interval. Designed an equipment to record the time domain damped oscillations response and further analysed to bring out the features that points the thickness change in stainless steel. A new method for analysis (Laplace domain or S-domain) has been imposed to ease the response data analysis and it clearly indicates the thickness change in S-domain. The results shows that the present analysis method can be a good candidate to represent the TECO data just like an impedance plane analysis of conventional ECT.

This work may be further implemented and this technic can be improvised by studying different case studies by performing numerical model based simulations and supporting experiments. By understanding the method more we can extract different feature to evaluate the test material condition.

Acknowledgement

This work is supported by the Department of Science and technology (DST), Science & Engineering Research Board (SERB) - India, under Early Career Research (ECR) Award project: ECR/2016/001790. The support has been greatly acknowledged.

References

[1] R. E. Melchers, Corrosion Sci. **81**, 110 (2014).
[2] K. Sathish Kumar and K. Balasubramaniam, J. Press. Vessel Technol.-Trans. ASME (2015).
[3] H. A. Kishawy, H. A Gabbar, International Journal of Pressure Vessels and Piping **87**, 373 (2010).
[4] Non-Destructive Testing for Plant Life Assessment. IAEA: Vienna (2005).
[5] R. Guilizzoni, G. Finch, and S. Harmon, IEEE Magn. Lett. **10**, 1 (2019).
[6] T. Chady, M. Enokizono, and R. Sikora, IEEE Trans. Magn. **35**, 1849 (1999).
[7] K. Sakai, K. Morita, Y. Haga, T. Kiwa, K. Inoue, and K. Tsukada, IEEE Trans. Magn. **51**, 1 (2015).
[8] A. Brysev, L. Krutyansky, O. Bou Matar, V. Preobrazhensky, and P. Pernod, In Proc. IEEE Ultrasonic Symposium, Montreal, QC, Canada, **3**, 2295 (2004).
[9] K. Sodsai, M. Noipitak, and W. Sae-Tang, In Proc. 7th International Electrical Engineering Congress (iEECON), Hua Hin **1**, 1 (2019).
[10] T Nelligan, Cynthia Calderwood, Introduction to Eddy Current Testing. https://www.olympus-ims.com/en/eddy-currenttesting/, accessed on 31 May 2021.
[11] C. C. Tai, Rev. Sci. Instrum. **71**, 3161 (2000).
[12] J. C. Moulder, M. W. Kubovich, E. Uzal, and J. H. Rose, In Rev of Progress in Quantitative Non-destructive Evaluation, 2065 (1995).
[13] J. Blitz and T. S. Peat, NDT E Int. **14**, 15 (1981).
[14] Lawal Umar Daura, GuiYun Tian, Qiuji Yi, and Ali Sophian, Philosophical Transactions A **378** 20190579 (2020).

[15] J. García-Martín, J. Gómez-Gil, and E. Vázquez-Sánchez, Sensors **11**, 2525 (2011).
[16] D. J. Pasadas, A. L. Ribeiro, T. J. Rocha, and H. G. Ramos, In Proc. 2014 IEEE Metrology for Aerospace, Italy **1**, 117 (2014).
[17] C. S. Angani, D. G. Park, C. G. Kim, P. Kollu, and Y. M. Cheong, J. Magn. **15**, 204 (2010).
[18] M. Djamal and Ramli, Procedia Engineering **32**, 60 (2012).
[19] C. S. Angani, H. G. Ramos, A. L. Ribeiro, T. J. Rocha, and B. Prashanth, Sens and Actu: A **233**, 217 (2015).
[20] Z. Zeng, P. Ding, J. Li, S. Jiao, J. Lin, and Y. Dai, Chin. J. Mech. Eng. **32**, 106 (2019).
[21] J. Kim, M. Le, J. Lee, and Y. H. Hwang, J. Nondest. Eval. **33**, 471 (2014).
[22] Liyuan Yin, Bo Ye, Zhaolin Zhang, Yang Tao, Hanyang Xu, Jorge R. Salas Avila, and Wuliang Yin, NDT and E Int. **107**, 102108 (2019).
[23] C. S. Angani, D. G. Park, C. G. Kim, P. Leela, and Y. M. Cheong, J. Nondestruct. Eval. **29**, 248 (2010).
[24] G. Y. Tian and A. Sophian, NDT E Int. **38**, 77 (2005).
[25] Y. He, G. Tian, H. Zhang, M. Alamin, A. Simm, and P. Jackson, IEEE Sens. J. **12**, 2113 (2012).
[26] T. Chen, G. Y. Tian, A. Sophian, and P. W. Que, NDT E Int. **41**, 467 (2008).
[27] W. Haowen, H. Jiangbo, L. Longhuan, Q. Shanqiang, and F. Zhihong, Sensors **22**, 614 (2022).
[28] Y. Song and X. Wu, Int. J. Appl. Electromagn. Mech. **64**, 1119 (2020).
[29] L. Udpa, W. Lord, and S. S. Udpa, In Rev of Prog in Quant Non-dest. Eval. 329 (1989).
[30] Q. Zhang, T. L. Chen, G. Yang, and L. Liu, Res. Nondestruct. Eval. **23**, 171 (2012).
[31] Yunze He, Mengchun Pan, Feilu Luo, and Guiyun Tian, NDT & E Int. **44**, 344 (2011).
[32] L. Lopez, D. Ting, and B. Upadhyaya, Progress in Nuclear Energy **50**, 828 (2008).
[33] S. Hosseini and A. A. Lakis, NDT & E Int. **47**, 70 (2012).
[34] https://en.wikipedia.org/wiki/LC_circuit, accessed on 31 May 2021.
[35] P. J. Shull, Nondestructive Evaluation: Theory, Techniques, and applications. Marcel Dekker, Inc., CRC Press (2002) pp 261-366.
[36] B. P. C. Rao, Practical Eddy Current Testing, Alpha Science Intl. Ltd. (2007).
[37] W. T. Thomson, Laplace Transformation. Prentice Hall (1960).